Trends in Analytical Chemistry 152 (2022) 116608

Contents lists available at ScienceDirect

Trends in Analytical Chemistry

journal homepage: www.elsevier.com/locate/trac

Molecularly imprinted polymers based optical fiber sensors: A review

Weiyingxue Yang [a], Yaxing Ma [a], Hui Sun [c], Chuixiu Huang [b, *], Xiantao Shen [a, **]

[a] State Key Laboratory of Environment Health (Incubation), Key Laboratory of Environment and Health, Ministry of Education, Key Laboratory of Environment and Health (Wuhan), Ministry of Environmental Protection, School of Public Health, Tongji Medical College, Huazhong University of Science and Technology, #13 Hangkong Road, Wuhan, Hubei, 430030, China
[b] Department of Forensic Medicine, Huazhong University of Science and Technology, #13 Hangkong Road, Wuhan, Hubei, 430030, China
[c] College of Environmental Science & Engineering, Guangzhou University, Guangzhou, Guangdong, 510006, China

ARTICLE INFO

Article history:
Available online 11 April 2022

Keywords:
Molecular imprinting
Optical fiber
MIP/OF sensor
MIP@OF sensor

ABSTRACT

Given the challenges facing on-site analysis, molecularly imprinted polymers (MIPs) based optical fiber (OF) sensors are earning worldwide attention because of their integration of high specificity (from MIPs) and flexible sensing ability (from OF sensors). As such, how to design an efficient MIPs based OF sensor becomes a timely research topic. In this review, we discuss the state-of-the-art of MIPs based OF sensors, including the simply combined MIP/OF sensors and the directly integrated MIP@OF sensors. We first summarize the progress of MIP/OF sensors using MIPs as solid phase extraction materials and binding films. In addition, we give a comprehensive overview of the MIP@OF sensors, with an emphasis on fluorescence, surface plasmon resonance (SPR), gratings, interferometry, lossy mode resonance and intensity distribution based MIP@OF sensors. Finally, the challenges and future perspectives of the on-site applications of these sensors are highlighted.

1. Introduction

On-site analysis using advanced sensors has attracted increasing attention in various fields including industry, agriculture, aerospace, biomedicine and environmental science. As a major branch of sensors, chemical sensors have been widely used in the detection of chemical and biological analytes in various sample matrices. Due to the fact that analytes usually present at trace level, chemical sensors should possess high selectivity and sensitivity during the applications. In this case, enhancing the specificity of the molecular recognition element in chemical sensors is particularly important.

One of the most efficient ways to address this challenge is the construction of recognition elements in chemical sensors with molecularly imprinted polymers (MIPs). It is known that MIPs are synthetic receptors generated by molecular imprinting [1]. Due to the physicochemical affinities between the functional groups of the template molecule and the functional moieties of the monomer, a template-monomer complex is first formed. After the polymerization and subsequent extraction, imprinted cavities (which are complementary to the template in size, shape and interaction points) are created. In comparison with other receptors, a distinctive nature of MIPs is the molecular recognition specificity. For this reason, molecular imprinting has emerged as a promising approach to enhance the target selectivity of chemical sensors [2].

Another type of sensors, optical fiber (OF) sensor, is also becoming a research focus for on-site analysis and remote sensing due to OFs' merits of miniaturization, portability, user-friendly operations, disposability, facile integration with various functional platforms, and availability at inaccessible sites (e.g., remote areas, strong magnetic fields and harsh environments), respectively [3]. These advantages provide the OF sensors with great potentials in practical sensitive responses towards electrical, mechanical [4] and chemical [5] parameters including strain, stress, magnetic field, current, temperature, vibration and chemical signals. In the literatures, a variety of sensing strategies of sensors have been demonstrated [6], including fluorescence, surface plasmon effect, interferometry, gratings, etc. Recently, with the development of functional materials (e.g., aptamer, enzyme and artificial antibody), OF sensors have also showed great feasibility in the detection of low-level chemical and biological analytes in various samples [7,8].

Thanks to the numerous advantages of molecular imprinting and OF technique, MIPs based OF sensors have been proposed. To date, they have attracted numerous attentions because of the high

* Corresponding author. .
** Corresponding author. .
E-mail addresses: chuixiuh@hust.edu.cn (C. Huang), xtshenlab@hust.edu.cn (X. Shen).

https://doi.org/10.1016/j.trac.2022.116608
0165-9936/

selectivity and great potentials for on-site analysis and remote sensing [9]. On the basis of the coupling methods between the MIPs and the OF sensors, we categorized them into simply combined MIP/OF sensors and directly integrated MIP@OF sensors. In the simply combined MIP/OF sensors, MIPs that were used for isolation of the analytes functioned independently in parallel with the OF sensors (as a detector). For the directly integrated MIP@OF sensors, MIPs were modified onto the optical fiber to fabricate the sensing platform. When the target analytes were bound onto this sensing platform, the optical properties of the MIP materials changed, which further resulted in the change of the wavelength, intensity, phase, or polarization state of the light signal (the intensity ratio change and wavelength shift per unit change in concentration of analytes are usually defined as sensitivity). In the literatures, the MIPs based OF sensor is proceeding rapidly in terms of its innovation and feasibility for on-site detection [10]. As such, how to design an efficient MIPs based OF sensor becomes a timely research topic.

Here, we summarize the current state-of-the-art of the simply combined MIP/OF sensors based on the two structural formats of MIPs: SPE column based and film based MIP/OF sensors. Then we give an integral overview of the directly integrated MIP@OF sensors. Beyond the thorough explanations of the sensor fabrication process concerning both MIP and OF preparation, we look into a wide range of sensing strategies including fluorescence, SPR, gratings, interferometry, lossy mode resonance and intensity distribution with the particular emphasis on the technical details and their effects on the performance. Finally, we discuss the challenges of the real-life applications of these sensors and envision the future perspectives in this field for achieving technological maturity.

2. Simply combined MIP/OF sensors

For sensors based on the simple combination of MIPs and OFs, MIPs served as the independent recognition element, while the OFs acted as the auxiliary of the detector to transmit light. Therefore, this type of MIPs based OF sensor was named MIP/OF sensor. The configuration of the MIP/OF sensors is flexible because the two parts of the sensors worked independently in the whole sensing process. So far, based on the structure of MIPs, there are two main formats reported: SPE column based MIP/OF sensors and film based MIP/OF sensors.

2.1. SPE column based MIP/OF sensors

Due to the high selectivity, effective enrichment and high potential for automation, MIPs based SPE (MIP-SPE) has been one of the most important sample pretreatment approaches. Other than conventional detectors (e.g., mass spectrometry), OFs based sensors were also used to measure the fluorescent target concentration in the MIP-SPE procedure. Thanks to the flexibility of the OFs based sensor, both the free target remaining in the solution after the adsorption and the bound target on the MIPs could be detected. For example, by connecting two OFs on each side of a flow cell where the effluent from the MIP columns flew through, the concentration of un-adsorbed analytes in the solution was determined by the transmitted absorbance spectra [11,12]. The same concept was also successfully applied in analyzing the adsorption behavior of MIP materials [13].

For the detection of the bound target on the column after the MIP-SPE procedure, the MIP columns could be coupled with the OF sensors [14] as well. As seen in Fig. 1a, with the O-ring as the connector between MIP-SPE columns and the end of the fiber, the excitation light from the light source and the fluorescence emission to the spectrometer could travel through the OF [14–16]. For example, using this SPE column based MIP/OF sensor, an on-line detection of the environmental pollutant was achieved with a limit of detection (LOD) of 1.38 μM [16].

The significant merit of this type of SPE column based MIP/OF sensor is that OFs and MIPs are separately established, the synthesis and performance of the MIPs and OF sensors are both controlled at the optimized conditions. However, so far, this format depends heavily on the optical properties of analytes, more effort is still needed for developing diverse sensing strategies to broaden its applicability.

2.2. Film based MIP/OF sensors

Regarding the film based MIP/OF sensors, MIPs as the recognition element in the sensor were modified onto the film. Besides fluorescence based OF sensors [17], localized surface plasmon resonance (LSPR), diffraction [18–22] and Raman [23] phenomenon based OF sensors were also coupled with the MIP film. The LSPR-based MIP/OF sensors required the layer of metal nanoparticle deposited below the MIP layer [24,25]. Encouragingly, with the high sensitivity of LSPR phenomenon to the changes of the MIP layer, gas sensing was achieved in both literatures. As for the diffraction-based MIP/OF sensors, colloidal crystal templating as the photonic element was widely applied with the MIP layer (Fig. 1b). It could produce reflected diffraction phenomenon [20] that could be recognized by spectrometer. Accordingly, Lai's group has achieved on-site detection in fish [21] and wine [22], with the detection LOD of 16.5 μg mL^{-1} and 10 μM, respectively.

As discussed above, OFs in the film based MIP/OF sensors played the roles of both excitation and recording. Due to OFs' advantages of miniaturization and ease of integration, composite films with proper optical properties can all be potential candidates of this type of format. Following this idea, we recently reported a fast and stable sensing system based on the MIP/OF format, which was capable of imaging Fe^{3+} in living cells [26].

For the MIP/OF sensors, their analytical performances depend on MIPs and the sensing strategy of OFs. Generally, the selectivity of MIP/OF sensors is mainly contributed by MIPs, while the sensitivity is dominated by the sensing strategy of OFs. Therefore, different degrees of focus should be placed on the optimization of MIPs and sensing strategies when developing MIP/OF sensors with different requirements. Moreover, concerning the instrumental set-up, OFs mainly act as a light transmitter with the ease of operation, which could be combined with a diversity of MIP formats (including particles [26,27]) and further enrich the application scenes (on-site or *in-vivo*) of MIP based optical sensors with different sensing strategies [2].

3. Directly integrated MIP@OF sensors

Integrating MIPs directly with OFs is a step towards the compactness and miniaturization of the MIP/OF sensor. In this concept, OFs serve as not only the optical transmission channel, but also the transduction element. Thus, this type of sensor is referred as MIP@OF sensor. When compared to simply combined MIP/OF sensors, the compatibility between MIPs and OFs should be of prior consideration. Thus, the options of MIPs are restricted in this regard, and the fabrication process of the sensors requires a high degree of elaboration. The performance parameters of all addressed MIP@OF sensors were tabulated in Table 1.

3.1. Fabrication of MIP@OF sensors

3.1.1. Modification of MIPs onto OFs

For all the MIP@OF sensors, the MIPs (layers or particles) were modified on the outset of OFs, serving to selectively recognize and

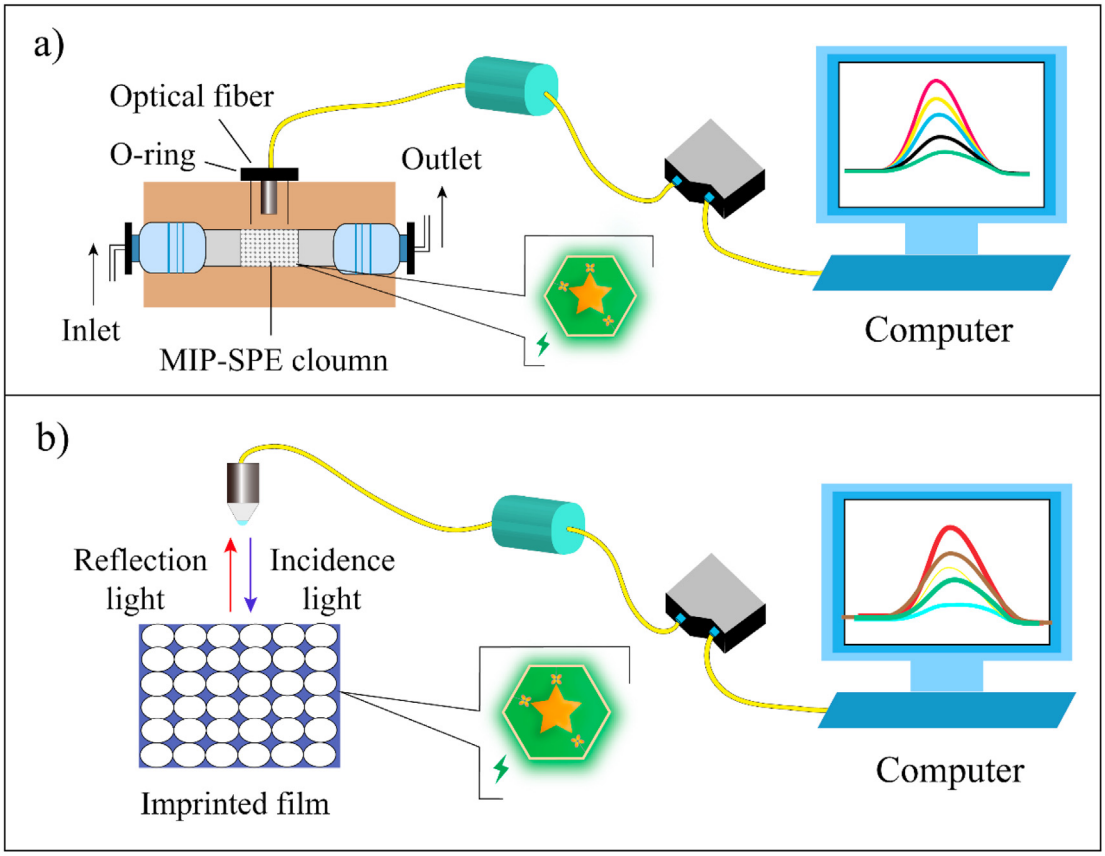

Fig. 1. Schematic illustrations of simply combined MIP/OF sensors. a) The experimental setup of SPE column based MIP/OF sensors; b) Experimental setup of film based MIP/OF sensors using diffraction as the sensing strategy.

capture the analytes in the samples. Generally, the modification approaches of the MIPs onto OFs include dip coating [59], drop coating [35] and spin coating [60]. Furthermore, considering the polymerized state of the imprinting ingredients during the modification, the modification of MIPs can be divided into 2 categories: *in-situ* polymerization method and post-polymerization method. For the *in-situ* polymerization method, pre-polymerization solutions were typically prepared by mixing the monomers, templates, cross-linkers, initiators and porogen solvents. By exposing to heat, light or electrons, the pre-polymerization mixtures were polymerized and *in-situ* coated onto the OFs. Among these polymerization methods, radical polymerization where azobisisobutyronitrile (AIBN) or ammonium persulfate (APS) were used as initiators was the most popular way. Photopolymerization was of practical significance because the experimental setup for the OFs could readily provide the light sources [58,61]. As for electropolymerization, it was helpful for obtaining controllable thickness of MIP layer to achieve plasmon signals in the case of SPR-based MIP@OF sensors [49]. Regarding the post-polymerization method, the MIP particles were synthesized before the modification process. The coupling of MIPs on the surface of OFs included physical adsorption and chemical grafting. The physical adsorption strategy was usually achieved through "gluing" MIPs onto OFs using hydrogels such as polyvinyl alcohol [62,63] and polyethyleneglycol diacrylate [34]. However, considering the destruction to the hydrogel structure by the high energy of the laser beam, the detection time should be restricted within seconds. Moreover, the stability pf the MIP@OFs by this physical adsorption method was unsatisfactory. One strategy to enhance the stability between the MIPs and the OFs was adding a metal layer between the MIP layers and OFs, which took the advantage of the electrostatic forces between the metal ions and MIP matrix, and was usually employed in SPR-based MIP@OF sensors [64]. To further increase the stability of the MIP@OF sensors, chemical grafting of OFs was carried out to obtain a chemically bound MIP layer. So far, vinyl group [29,47] and amino group [48,51,55,65] based silane coupling agents were used. Besides, the chemical grafting of OFs with a layer of nanoparticles (e.g., SiO_2 nanoparticles) was also reported to provide high surface area for the MIP modification [52].

In short, the *in-situ* polymerization method requires less experimental operation, and the light source for the detection can readily facilitate the polymerization process. Nevertheless, it still remains a challenge to manage the polymerization condition so that OF sensors are reproducible in industrial-scale production [48]. For the post-polymerization method, it shows the disadvantage of more handling procedures. Besides, homogenous coating of MIP materials onto OFs should be of primary concern for enhancing the performance and stability of the sensors [28,34,63].

3.1.2. Generation of sensing platform on OFs

The commercialized OFs are generally made of plastic (POFs) or silica (SOFs). In comparison, the SOFs are superior in providing high-bandwidth and low-loss long-distance transmission in harsh environment and are more widely used [66], while the POFs are more resilient, more bio-friendly, lighter, cheaper and have huge potential in low-cost and *in-vivo* applications [60]. Especially, when the disposability is among the priorities when developing an on-site sensor, POFs can be a nice candidate [62,63]. To construct a MIP@OF sensor using the commercialized OFs, a sensing platform is needed on the OFs. At the sensing platform of MIP@OFs, the binding

Table 1
Performance parameters of MIP@OF sensors.

Sensor	Analyte	Sample	Incubation time	LOD	Sensitivity	Range	Ref.
Fluorescence	Organophosphates	Water	14 min	5×10^{-6} mg L^{-1}		5×10^{-6}-100 mg L^{-1}	[28]
	Cocaine	Water	15 min	2×10^{-6} M		0–5×10^{-4} M	[29]
	2,4-D	Water	10 min	2.5×10^{-9} M		0–2.5×10^{-8} M	[30]
	Bisphenol A	Water	2 min	1.7×10^{-3} mg L^{-1}		3×10^{-3}-5 mg L^{-1}	[31]
	Enrofloxacin	Serum	> 60 min	4×10^{-8} M		2.9×10^{-7}-2.154×10^{-5} M	[32]
	D-aspartic acid	Water	–	1.8×10^{-6} M		0-10^{-5} M	[33]
	Ciprofloxacin	Water	30 min	6.86×10^{-6} M		10^{-5}-5×10^{-4} M	[34]
SPR	Vitamin B3	Water	40 s	–	1.483×10^{-3} nm L mg^{-1}	0–10^{4} mg L^{-1}	[35]
	L-nicotine	Water	10 min	1.86×10^{-4} M	1.3×10^{4} nm M^{-1}	0-10^{-3} M	[36]
	TNT	Water	5 min	7.2×10^{-7} M	8.3×10^{5} nm M^{-1}	0-10^{-4} M	[37]
	Atrazine	Water	–	1.92×10^{-14} M	21.99 nm log^{-1} M	0-10^{-7} M	[38]
	Melamine	Water	–	9.87×10^{-9} M	–	10^{-7}-10^{-1} M	[39]
	Tetracycline	Water	40 s	2.2×10^{-9} M	1.5×10^{8} nm M^{-1}	10^{-8}-10^{-5} M	[40]
	Ascorbic acid	Water	< 5 s	7.383×10^{-11} M	45.1 nm log^{-1} M	10^{-8}-10^{-6} M	[41]
	Erythromycin	Water	< 15 s	1.62×10^{-9} M	2.05×10^{8} nm M^{-1}	1.62×10^{-9}-10^{-4} M	[42]
	Serum transferrin	Water	10 min	1.2×10^{-15} M	–	1.2×10^{-15}-1.8×10^{-12} M	[43]
	Perfluorooctanoate	Water	10 min	1.3×10^{-4} mg L^{-1}	2.214×10^{4} nm L mg^{-1}	0–4×10^{-3} mg L^{-1}	[44]
	Dopamine	Cerebrospinal fluid	10 s	1.89×10^{-11} M	68.58 nm log^{-1} M	0-10^{-5} M	[45]
	Furfural	Wine	5 min	0.004 mg L^{-1}	254.9 nm L mg^{-1}	0–5.8 mg L^{-1}	[46]
Gratings	Maltol	Jelly	10 min	8.1×10^{-9} M	6.3×10^{5} nm M^{-1}	0-10^{-6} M	[47]
	Vancomycin	Plasma	45 min	1.8×10^{-9} M	–	10^{-8}-7×10^{-4} M	[48]
	Formaldehyde	Gas	–	–	2.1×10^{-3} nm L mg^{-1}	–	[49]
	TMPyP	Water	15 min	–	–	0-10^{-4} M	[50]
	Carboxyl-fentanyl	Water	20 min	0.05 mg L^{-1}	–	0–1 mg L^{-1}	[51]
	Creatinine	Urine	5 min	10^{-5} M	200 nm M^{-1}	0–0.025 M	[52]
Interferometry	Microcystin-LR	Water	2 min	–	1.24×10^{4} nm L mg^{-1}	3–14×10^{-4} mg L^{-1}	[53]
	Parathion Methyl	Water	1 min	7.943×10^{-14} M	1.3×10^{12} nm M^{-1}	10^{-12}-10^{-4} M	[54]
	C-reactive protein	Water	30 min	5.813×10^{-13} mg L^{-1}	0.88 nm log mL ng^{-1}	10^{-13}-10^{-5} mg L^{-1}	[55]
LMR[a]	Cortisol	Saliva	20 s	2.59×10^{-8} mg L^{-1}	12.8 nm log mL g^{-1}	10^{-5}-0.1 mg L^{-1}	[56]
	p-Cresol	Urine	15 s	2.8×10^{-8} M	1.186×10^{7} nm M^{-1}	0-10^{-3} M	[57]
Intensity	Dibenzyl disulfide	Oil	5 min	5.3×10^{-8} M	5.2×10^{5} M^{-1}[b]	5.3×10^{-8}-2×10^{-6} M	[58]

[a] Lossy mode resonance.
[b] Defined as intensity ratio change per unit change in concentration of analytes.

of analytes can induce the changes of the optical properties of the MIP layer. When these changes are transmitted or transduced into optical signals (e.g., intensity change, wavelength or phase shifts) by different sensing strategies, the OFs subsequently deliver the signals to the spectrometers for quantification of the analyte concentration. Therefore, in order to introduce the light propagating from the core of the OFs to the MIP layer, it is necessary to treat the sensing area of the OFs before the MIP modification, which is a vital manufacture process influencing both the performance and practicability of the MIP@OFs.

There are four methods for outcoupling light into the MIP layer: tip modification, uncladding, U-bent and grating (Fig. 2) [7], all of which are designed on a small segment of OFs (point sensing/sensing platform) [67]. It is seen in Fig. 2c that the fiber tip modification was achieved by depositing MIPs on the distal end of OFs without altering the light's direction. Two types of MIP@OF sensors have been proposed using the tip modification. One was the MIP@OF sensor based on Fabry-Pérot interferometer, which transferred the refractive index (RI) change of the MIP tips into the wavelength shift of the interferometric spectra [53]. Another intriguing one was the fluorescence-based MIP@OF sensor with a core-shell microtip [30]. In this method, OFs were cleaved at one end of the tips, and then a drop of polymer was formed as both the support and transducer element for the successive deposition of MIP layer. This strategy of microtip accelerated both the polymerization and detection.

As a second method for outcoupling light into the MIP layer (Fig. 2a), the uncladding was to remove the cladding of OFs around [64] or along half [68] of its circumference at the sensing region. In this case, it was the evanescent wave rather than the original propagating light that reached out to contact with the MIP layer. Most of the sensing strategies required the uncladding to achieve proper sensitivities to the external signal alteration [69], except for gratings-based MIP@OFs [49]. As the third method for introducing light outside the OF cores, the inscription of a periodic grating structure onto the core of OFs was requisite. Most commonly used gratings included tilted fiber Bragg gratings (TFBGs) and long-period gratings (LPGs) (Fig. 2d). Since the uncladding process was exempted from this method, the mechanical strength of OFs was preserved. It is noted that "U-bent" method (Fig. 2b) has not been reported in MIP@OF sensors due to the difficulties in modifying the MIP element onto the curved section of OFs.

3.2. Fluorescence-based MIP@OF sensors

3.2.1. Concept of quantitative analysis

Fluorescence MIP@OF sensor is the most common type in non-functional MIP@OF sensors. The rationale of all the fluorescence-based MIP@OF sensors is the alteration of fluorescence intensity before and after the sensing. So far, three different sensing concepts have been reported: directly quantitative analysis of the fluorescent analyte itself (Fig. 3a), fluorescence change (enhancement) of the MIP fluorophore by the non-fluorescent target binding (Fig. 3b), displacement of a fluorescent analogue by the non-fluorescent analyte binding (Fig. 3c). The first concept of quantitative analysis is the simplest way and requires the easiest setup. Research exploring the fluorescent analytes has been reported recently, where the detection of the antibiotic ciprofloxacin relied on its strong fluorescence under the excitation at 400 nm [34]. Using this fluorescence-based MIP@OF sensor, a detection limit of 6.86 μM was achieved for the target ciprofloxacin. Beside ciprofloxacin, bisphenol A with the excitation and emission wavelength at 276 nm and 306 nm has also been selected as the analyte [31]. There are two main disadvantages presented in this type of fluorescence

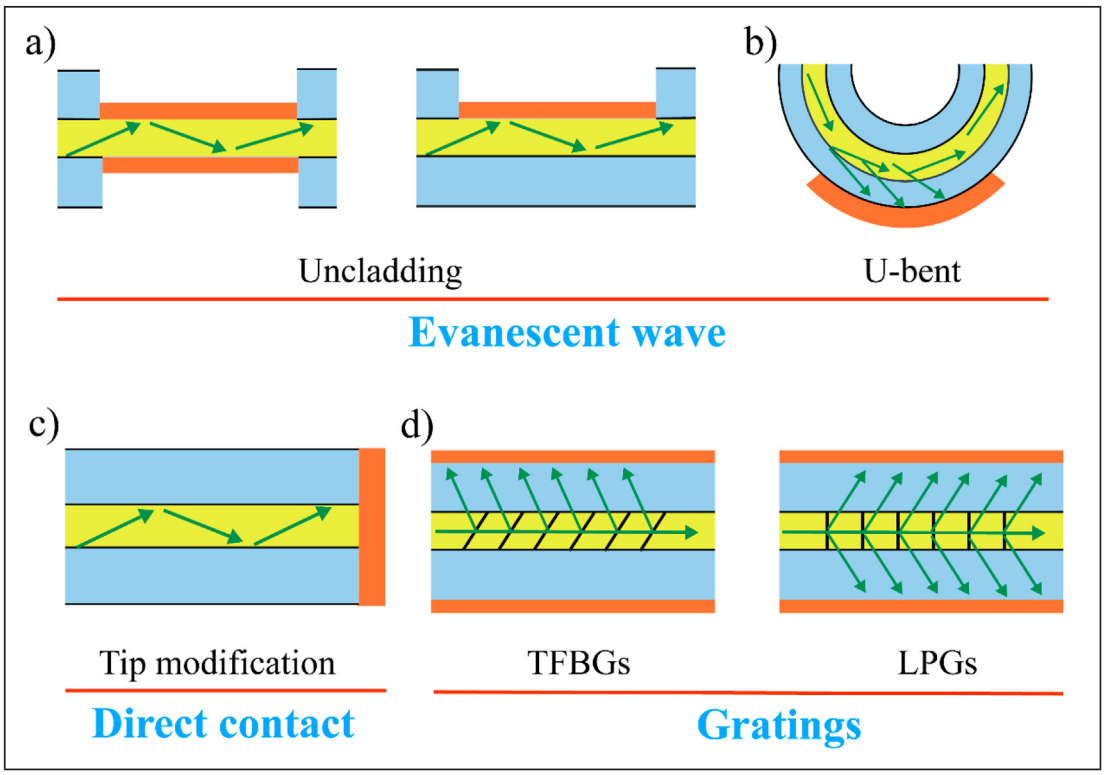

Fig. 2. Schematic illustrations of methods for generation of sensing platform on OFs: a) uncladding, b) U-bent, c) tip modification and d) gratings. (Adapted from Ref. [7]. Copyright (2021), Elsevier.).

MIP@OF sensor. One is that only a limited variety of the analytes bear the satisfactory fluorescent properties. The other is that necessary steps to rinse and relocate the MIP@OF sensor after the adsorption process to eliminate the background fluorescence from the sample are time-consuming. The second concept for quantitative analysis is the fluorescence enhancement of the MIP fluorophore by the non-fluorescent target binding. The presence of the fluorophore in the MIPs is originated from the use of fluorescent monomers or additional fluorescent component during polymerization. So far, the fluorescent monomers for the generation of MIPs on the MIP@OF sensors included acrylamidofluorescein (AAF) [29,70], perylene bisimide monomer (PBIM) [33], *N*-2-(6-(4-methylpiperazin-1-yl)1,3-dioxo-1H-benzo[de]isoquinolin-2(3H)-yl-ethyl)acrylamide (FIM) [30,63]. Besides the fluorescent monomers, Europium as a luminescent lanthanide was the only additional fluorescent component that have been incorporated into the MIP@OF senor build-up. The luminescent lanthanide not only functioned as a signal transducer, but also strengthened the affinity of the MIPs toward the templates [28]. The third mechanism for quantitative analysis is the displacement of a fluorescent analogue by the non-fluorescent analyte binding. In order to quantify the target's concentration, competitive binding experiments with the addition of target's analogue as the fluorescent probe are cumbersome [30]. There was an intriguing report about an immuno-like MIP@OF sensing array for antibiotic analysis [32]. Though the manufacture of the MIP@OF sensor in this work was formidably complex, it proved the potentials of MIP@OFs as biomimetic sensors for multiplexed detection.

3.2.2. Configurations

As seen in Fig. 3d and e, the basic instrumental setups of fluorescence-based MIP@OF sensors include the light source, MIP@OFs, the spectrofluorometer and optical spectrum analyzer. Besides the MIP layers that are designed according to the research interests, two sensing setups have been reported regarding how the fluorescence travels to the spectrofluorometer: by another fiber (transferring) (Fig. 3d) and by the same fiber (backtracking) (Fig. 3e). "Transferring" requires an external fiber optic spectrofluorometer to capture the fluorescent emission, which is released from a confined area like a fiber tip or a cuvette, and transferred to the spectrometer by the connector-terminated OFs. In 2013, Haupt's group reported the MIP-coated microtip to facilitate faster manufacture (within seconds) and sensing response (10 min of incubation) [30]. However, applying "transferring" leads to extra steps such as retrieving fibers from the analyte solution and installing the fiber probes into the spectrometer, which restrict the applicability in on-site and remote monitoring. Therefore, future miniaturization such as microfluidic sensor chips [30] could enhance the fluorescence signal transmission and thus exempt sensors from the need of multi-steps "transferring". Accordingly, an on-line system which could serve as the reference for realizing future miniaturization was proposed by Xiong et al. [31]. In this study, the MIP@OF sensor was fixed in a capillary tube where sample solutions and elusion solutions passed through. The fluorescence detector fixed outside the tube could record the signals without further manual operations. For "backtracking", both excitation injection and fluorescence collection are realized through the Y-shaped bifurcated fiber probe. So far, fluorescence-based MIP@OF sensors with Y-shaped OFs have been widely used for quantitative detection [29,30,34,63,70]. By controlling the fluorescence signals to travel back through the same fiber, the detection suffers less from the ambient interferences. Therefore, low-background and direct detection while the probe remained in the analyte solution were achieved [63]. This type of configuration is conducive to the remote real-time detection, because the Y-shaped fiber breaks the length confinement of the fiber probe with an extra

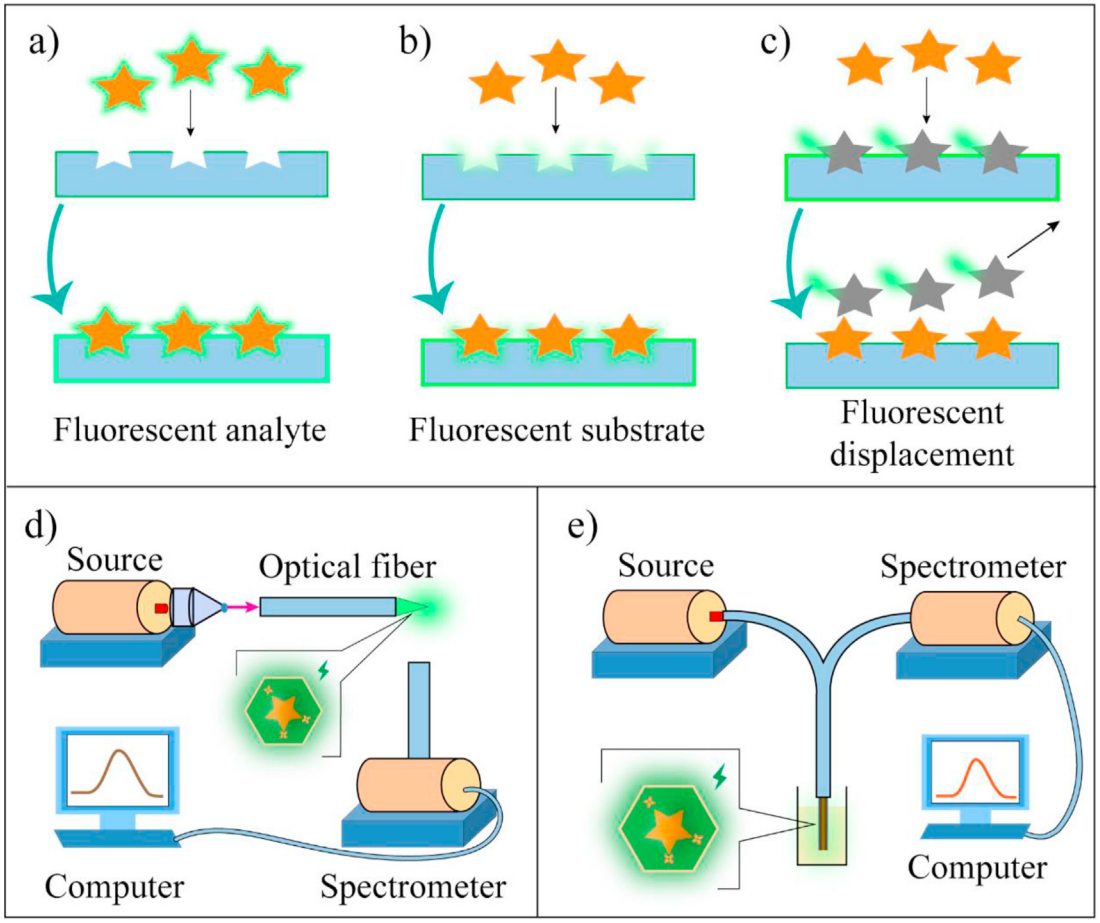

Fig. 3. Schematic illustrations of concepts of quantitative analysis by a) fluorescent analyte, b) fluorescent monomer and c) fluorescent analogue; Schematic illustrations of two configurations of fluorescence-based MIP@OF sensors, including d) transferring and e) backtracking. (Adapted from Ref. [38]. Copyright (2015), Elsevier).

fiber arm, and the operation of the detection is user-friendly. Other than these merits, the disposability of the probe was first achieved by the flange adapter in our group [34]. The introduction of the flange adapter facilitated the facile detachment and replacement of the fiber probe.

It is seen from Table 1 that the major drawback of the fluorescence-based MIP@OF sensors is their relatively long incubation time, which prevents significantly their applicability in on-site real-sample detection. As a method to overcome this challenge, the concept of "microtip" might be an efficient way to speed up both the manufacture and testing process.

3.3. SPR-based MIP@OF sensors

3.3.1. Sensing mechanism and setup

Due to its ultra-sensitivity, fast response and versatility, SPR technique has proved its prime reliability and applicability in the detection of copious chemical and biological agents [35,71]. In order to produce OF sensors for on-site detection, SPR technique can be an excellent choice. The according sensing mechanism focuses on the surface plasmons at the metal-dielectric interface, where a metal layer is sprayed between the MIP layers and OFs, and MIP layers serve as the dielectric interface in the case of SPR-based MIP@OF sensors. When the evanescent wave of the incident light of a certain wavelength matches the surface plasmon wave, a significant transfer of the energy from the incident photons to the surface plasmons will happen, which leads to a sharp dip (resonance wavelength) on the SPR spectrum. Since the resonance wavelength is affected by the RI of the MIP layer (which changes upon the binding of different amounts of analytes), the alteration of the resonance wavelength is thus determined by the function of analyte concentration change. The detailed elaboration can be found in the previous review by Sharma et al. [72].

In regard with the instrumental setup, SPR-based sensors have the similar configuration (light source, MIP@OFs and spectrometer) as that of the fluorescence-based MIP@OF counterpart. Besides, SPR-based sensors also carry the merits of low sample requirement and short incubation time due to its ultra-sensitivity towards the RI of the MIP layer. In the literature, SPR-based MIP@OF sensors were reported to fulfill the detection by the minimum sample requirement of $\leq$100 μL [60,68]. The time required for recording the SPR spectra was usually less than 5 min, which is rather practically competent compared to the fluorescence-based MIP@OF sensors regarding the on-site application. Encouragingly, Cennamo et, al has reported a proof of concept of the SPR-based MIP@OF sensor for fast on-site SARS-CoV-2 detection that took around 10 min [10]. Regarding the on-site application, it is possible for all components of the instrument to be compacted and miniaturized with satisfactory robustness. The graphic sketch of the according setup is shown in Fig. 4a. However, unlike spectrofluorometers, the spectrometers for SPR signals are more expensive regarding the manufacture and maintenance [34].

3.3.2. Improved performance of SPR-based MIP@OF sensors

There are several strategies reported in the literatures to improve the detection performance of SPR-based MIP@OF sensors. Similar as other types of MIP@OF sensors, tapering is the most basic strategy by altering the sensors' geometry. As an important indicator of the performance of MIP@OF sensors, sensitivity (defined by the resonance wavelength shift per unit change in concentration of analytes) was reported to increase 10 times after the tapering [37]. Likewise, higher taper ratio (the diameter of the tapered region/original diameter of the OF) brought about higher sensitivity as well [36]. LSPR is another well-researched type of surface plasmon phenomenon. Rather than spreading across the metal-dielectric

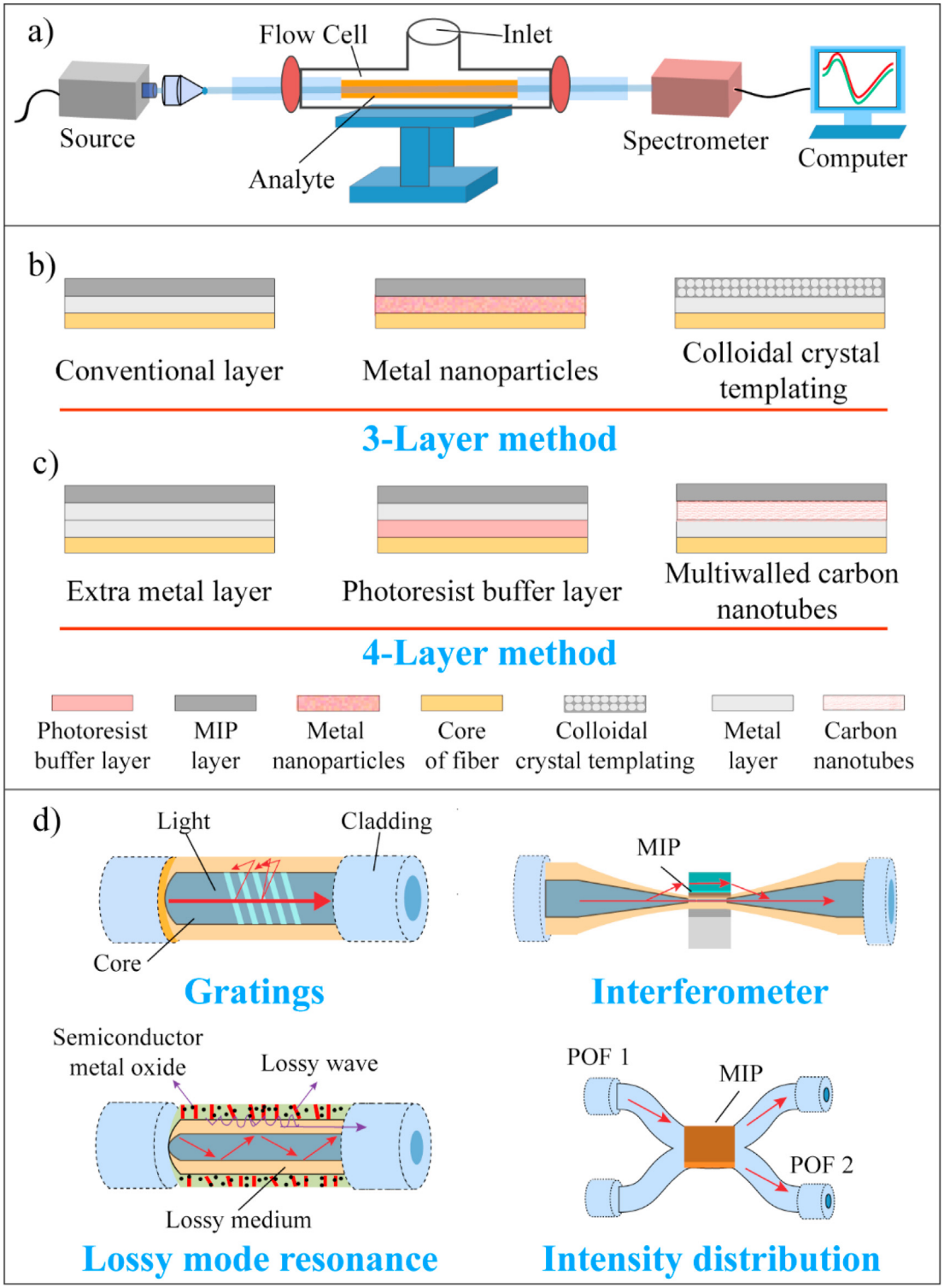

Fig. 4. Schematic illustrations of a) typical experimental setup of SPR-based MIP@OF sensors (Adapted from Ref. [38]. Copyright (2015), Elsevier.); b) 3-layer method; c) 4-layer method for performance improvement of SPR-based MIP@OF sensors; d) other MIP@OF sensors based on gratings, interferometry, LMR and intensity distribution. (Adapted from Ref. [56]. Copyright (2017), Elsevier.).

interface, the oscillation of electrons is confined in metal nanostructures (Fig. 4b), leading to the enhancement of the electric field [71]. Together with the larger interaction surfaces between the metal and MIP layer provided by the nanostructures, the LSPR-based sensors were endowed with higher sensitivity and lower LOD compared to its SPR counterpart [37]. With this strategy, gold nanostars and silver nanoparticles [40,41] based MIP@OF sensors have been designed. Encouragingly, the highest sensitivity of the SPR-based MIP@OF sensor for ascorbic acid reached 45.1 nm $\log^{-1}$ M [41]. Besides the change of the metal layer, change of the MIP layer in the SPR-based MIP@OF sensor could also increase the performance of the sensors. Recently, "colloidal crystal templated" imprinted layer prepared by tridimensional packed monodisperse polystyrene nanospheres in the imprinting system was reported to enhance the binding performance of the MIP layer by providing higher surface area and spatial binding sites for MIPs (Fig. 4b). The sensitivity of the SPR-based MIP@OF sensor was accordingly found to be 1.483×10^{-3} nm L mg^{-1}. Moreover, the analyte-triggered deformation of the MIP layer as a novel perspective of performance optimization was recently proposed by Cennamo et al., which brought the LOD of the SPR-based MIP@OF sensor to as low as 1.2 fM [43]. Moreover, other strategies related with improving the performance of the SPR-based MIP@OF sensor have been proposed by inserting an extra layer of materials (Fig. 4c). For example, a photoresist buffer layer was deposited between the metal layer and OFs [44,60,61,68], which functioned like another metal layer to enhance the detection sensitivity of the sensor [73]. Between the metal and MIP layer, an aluminum layer was also inserted to increase the sensor sensitivity by absorbing more light and creating larger shift in the resonance wavelength [38,39]. Similarly, an extra layer of multiwalled carbon nanotubes between the metal and MIP layer could boost the charge transfer reaction at the metal/MIP interface, by which a LOD of 18.9 pM was achieved [45].

In brief, compared to the fluorescence-based MIP@OF sensors, coupling the SPR phenomenon with MIP@OF sensors is promising due to the less sample requirement, faster detection and high sensitivity (Table 1). However, besides the higher cost for maintenance, the other drawback might be that the metal applied might face corrosion for long time usage in the harsh aqueous environment [6].

3.4. Other MIP@OF sensors

3.4.1. Gratings-based MIP@OF sensors

Optical fiber gratings are another strategy of MIP@OF sensors that is about the transduction of the changes of the RI of MIP layers. The basic principle of gratings is that periodical RI modulation of OFs' cores can lead to the backward/forward reflection of a certain wavelength that is in phase with the grating period (Fig. 4d). Thus, a dip called "resonance wavelength" on the transmission spectra will be observed, which is decided by the effective RI of the OF cores and sensitive to some physical parameters including temperature [74]. In order to detect the changes of the surrounding RI, two types of gratings have been introduced to MIP@OF sensors including TFBGs and LPGs. Both grating methods are designed to lead the light outside to reach the interface between the cladding of OFs and outer medium. Therefore, the resonance wavelengths where the coupling happens between the core modes and clad modes also depend on the surrounding RI that affects the effective RI of the core mode [74], realizing the detection of the RI changes of MIP layers when encountering with different concentrations of analytes. As discussed above, one of the merits of grating-based MIP@OF sensors is the exemption of uncladding procedures. However, inscription of grating planes onto OFs with laser is necessary, which could be lengthy together with the successive dehydrogenization in some cases [49], thus perplexing and increasing the cost of the fabrication process. Meanwhile, since the grating period of LPGs (100 μm−1 mm) is much larger than that of FBGs (<1 μm), the fabrication is generally much easier for LPGs.

Upon applying LPG-based MIP@OF sensors, its especially high sensitivity to the ambient temperature should be considered when detecting the analytes concentration changes [62]. Therefore, other than the typical singular configuration [48], double-LPG configuration has been proposed recently, in which one LPG acted as a reference for the calibration of temperature [51]. In this study, the LOD of 50 ng mL^{-1} was achieved. Notably, due to its core-cladding mechanism, optical fiber gratings can also be integrated with SPR-based sensors. The according concept has been realized on the hybrid TFBG-SPR MIP@OF sensor by Álvaro González-Vila and colleagues [49]. In the study, TFBG was adjusted to incite the SPR phenomenon, which increased the refractometric sensitivity of SPR's signal. As a result, the TFBG-SPR MIP@OF sensor achieved the detection of formaldehyde in gas, which further broadened the application scenes of MIP@OF sensor. The sensitivity of the sensor was 2.10×10^{-3} nm L mg^{-1}. Recently, we reported that the molecularly imprinted TiO_2 photocatalysts were efficient for decomposition of the bound target pollutants on the MIPs [75]. Similarly, Wang et al. fabricated the imprinted TiO_2 nanofilm towards Tetrakis(*N*-methylpyridinium-4-yl)porphyrin (TMPyP) onto the LPG-based MIP@OF sensor to realize the self-cleaning feature of the sensor [50]. This work further enriched the potentials of gratings-based MIP@OF sensors in highly automated on-site and remote applications.

To date, the quantitative detection of gratings-based MIP@OF sensors has been realized on water [50], jelly [47], porcine plasma [48], and gas [49]. However, rather low sensitivity and high cost of the fabrication are the main hurdles on its way for future on-site application.

3.4.2. Interferometry-based MIP@OF sensors

Interferometry-based MIP@OF sensors exploit the interference phenomenon between two lights that share the same frequency and transmission direction with the constant phase difference [6]. One phase of the lights is affected by the RI of the sensing medium, while the other remains unaffected as the fundamental mode. Therefore, the effective phase difference of two lights changes due to the RI change of the sensing element, which further leads to the shift of the interference spectra. Generally, the dip wavelength of the interference spectra is used for analyzing the shift.

Two configurations of the interferometry-based MIP@OF sensors have been proposed. The first one was based on the Fabry-Pérot interferometer with a simple fabrication process [53]. This type of interferometer-based MIP@OF sensors utilized the partially reflective end of the fiber (fiber tip method) with the MIP layer and an external mirror to create the interference between the reflected lights. In this configuration, the design of the sol-gel feature of the MIP layer was of critical importance because of its transparency in the visible region, which allowed the pass of incident lights. Thus, the effective phase difference between two lights was decided by the thickness and the RI of the sol-gel MIP layer [76]. The resulted sensor presented a detection sensitivity of 1.24×10^4 nm L mg^{-1} towards the target analyte. Besides, this sensor showed low thermal cross-sensitivity. Another configuration based on the Mach-Zehnder interferometer involved the tapering process (Fig. 4d). The design was to fabricate regions of microfibers produced by tapering between the non-tapered regions, which introduced the evanescent wave into cladding modes at tapered region and then redirected it back at non-tapered region, resulting in the interferences [77]. Accordingly, Liu et al. prepared the interferometry-based MIP@OF sensor with a single tapered region (with a diameter of 7.30 μm) [55]. Notably for the sensor, ultra-

sensitivity and LOD of 0.881 nm lg mL ng^{-1} and 5.813 $\times$ 10^{-10} ng mL^{-1} respectively were achieved, which outperformed the commercial sandwich-type ELISA kit by a huge margin. Recently, Shrivastav et al. also developed an interferometry-based MIP@OF sensor with concatenated tapered-regions (with a diameter of 10 μm), which were to maintain the stable interference pattern while the RI of MIP layer increased too largely [54]. Similarly, the detection method based on this sensor realized the ultra-sensitivity and LOD of 1.30 $\times$ 10^{12} nm M^{-1} and 79.43 fM, respectively.

However, though the Mach-Zehnder interferometer-based sensors yield a better sensor performance with the miniaturized structure, their mechanical strength is compromised by the tapering process. Generally, compared to the grating-based counterpart, the interferometry-based MIP@OF sensors show higher sensitivity as well as more flexible fabrication process [6,78].

3.4.3. Lossy mode resonance MIP@OF sensors

Lossy mode resonance (LMR) technique is another promising counterpart of SPR that shares the similar configurations, for which the metal layer in SPR setup is instead switched into a layer of metal oxides, polymer coatings or organometallics in LMR (Fig. 4d) [79]. In the two studies of LMR-based MIP@OF sensors, a layer of semiconductor metal oxide was applied, to which a part of the core modes was lost. The LMR then happened when the lossy modes that were sensitive to the RI change of MIP layer coupled to the guided modes in the OF's core. Thus, a dip in the transmission spectrum was observed as the resonance wavelength shifts when the phase of lossy modes changes following the RI change of the MIP layer. In the pioneer studies of Gupta's group, the sensitivity and LOD of 1.186 $\times$ 10^{7} nm M^{-1} and 28 nM respectively were achieved for the urinary *p*-cresol diagnosis with this LMR-based MIP@OF sensor [57]. For the cortisol analysis in the artificial saliva, LMR-based MIP@OF sensor showed a LOD of 25.9 fg mL^{-1} [56]. Nevertheless, the study of LMR technique in OF sensors is still in the preliminary stage, yet its continuous advancement indicates that the LMR technique can be a prospective candidate for future sensor development.

3.4.4. Intensity-based MIP@OF sensor

Other than the typical refractometric sensors, there was one study that focused on transducing the RI change into the signal's intensity change [58]. The configuration of the sensor was rather simple, with two OFs placed in tight contact and a trench further carved on top of them for the deposition of MIPs as the sensing platform, resulting in the formation of two adjacent segmented waveguide sensors (SWS) (Fig. 4d). The sensing mechanism of SWS was based on the modal mismatch, by which the incident light passing through one OF was distributed partially to the other OF. The degree of this power distribution depended on the properties of the sensing segment. Higher RI of the segment led to the higher power distribution that could be denoted as the intensity ratio between the two OFs. With this configuration, an on-site detection of the target analytes in oil phase was achieved with a detection LOD of 5.3 $\times$ 10^{-8} M. Even though intensity-based MIP@OF sensors still require further research, its fairly easy fabrication process is attractive for developing facile and low-cost sensors.

4. Conclusions and perspectives

In this paper, the MIPs based OF sensors including the simply combined MIP/OF sensors and directly integrated MIP@OF sensors have been comprehensively reviewed. For the MIP/OF sensors, the independent functions of MIPs and OFs provide the sensor with abundant choices regarding its construction. However, based on the current progress of the MIP/OF sensors, it is seen that the limitations of detectable analytes for SPE column based MIP/OF sensors still exist, while film based MIP/OF sensors are more versatile regarding sensing strategies. Nevertheless, more formats like nanoparticles based MIP/OF sensors should be exploited for future on-site applications. We then gave a comprehensive overview of the directly integrated MIP@OF sensors. We elaborated the sensor fabrication by looking into the methods for modifying MIPs onto OFs and generating sensing platforms on OFs. The configurations and applicability of each sensing strategies were also highlighted.

Aside from great potentials of the MIPs based sensors for on-site analysis, following challenges and perspectives for future research are given: i) Besides the conventional MIPs functioned as the recognition element in the sensors, “smart” MIPs can be further developed to possess merits like self-cleaning and stimuli-responsiveness; ii) Considering the aqueous property of the majority of environmental and biological samples, developing hydrophilic MIPs while considering the facileness of modifying MIPs onto OFs is of vital significance; iii) Each sensing strategies have distinct advantages and disadvantages, the coupling of two or more sensing strategies might lead to better performances.

So far, commercialized MIPs based sensors are still lacking. From this aspect, all the above sensors are still within the stage of basic scientific research, thus the sensing setups should be further miniaturized, compact and easy to operate while keeping the balance between efficiency and robustness for realizing the real “on-site” application.

Declaration of competing interest

The authors declare that they have no known competing financial interests or personal relationships that could have appeared to influence the work reported in this paper.

Acknowledgements

This work was supported by the National Natural Science Foundation of China (21874050) and the National Key Research Development Project of China (2019YFC1804504).

References

[1] R. Xing, S. Wang, Z. Bie, H. He, Z. Liu, Preparation of molecularly imprinted polymers specific to glycoproteins, glycans and monosaccharides via boronate affinity controllable-oriented surface imprinting, Nat. Protoc. 12 (2017) 964–987. https://doi.org/10.1038/nprot.2017.015.
[2] O.S. Ahmad, T.S. Bedwell, C. Esen, A. Garcia-Cruz, S.A. Piletsky, Molecularly imprinted polymers in electrochemical and optical sensors, Trends Biotechnol. 37 (2019) 294–309. https://doi.org/10.1016/j.tibtech.2018.08.009.
[3] I. Floris, J.M. Adam, P.A. Calderón, S. Sales, Fiber optic shape sensors: a comprehensive review, Opt Laser. Eng. 139 (2021) 106508. https://doi.org/10.1016/j.optlaseng.2020.106508.
[4] D. Cao, H. Zhu, C. Guo, J. Wu, B. Fatahi, Investigating the hydro-mechanical properties of calcareous sand foundations using distributed fiber optic sensing, Eng. Geol. 295 (2021) 106440. https://doi.org/10.1016/j.enggeo.2021.106440.
[5] M. Yin, B. Gu, Q. An, C. Yang, Y. Guan, K. Yong, Recent development of fiber-optic chemical sensors and biosensors: mechanisms, materials, micro/nano-fabrications and applications, Coord. Chem. Rev. 376 (2018) 348–392. https://doi.org/10.1016/j.ccr.2018.08.001.
[6] Y. Qian, Y. Zhao, Q. Wu, Y. Yang, Review of salinity measurement technology based on optical fiber sensor, Sensor. Actuator. B Chem. 260 (2018) 86–105. https://doi.org/10.1016/j.snb.2017.12.077.
[7] M. Loyez, M.C. DeRosa, C. Caucheteur, R. Wattiez, Overview and emerging trends in optical fiber aptasensing, Biosens. Bioelectron. 196 (2022) 113694. https://doi.org/10.1016/j.bios.2021.113694.
[8] J. Svitel, I. Surugiu, A. Dzgoev, K. Ramanathan, B. Danielsson, Functionalized surfaces for optical biosensors: applications to in vitro pesticide residual analysis, J. Mater. Sci. Mater. Med. 12 (2001) 1075–1078. https://doi.org/10.1023/A:1012810527291.
[9] L. Jiao, N. Zhong, X. Zhao, S. Ma, X. Fu, D. Dong, Recent advances in fiber-optic evanescent wave sensors for monitoring organic and inorganic pollutants in

water, Trends Anal. Chem. 127 (2020) 115892. https://doi.org/10.1016/j.trac.2020.115892.
[10] N. Cennamo, G. D'Agostino, C. Perri, F. Arcadio, G. Chiaretti, E.M. Parisio, G. Camarlinghi, C. Vettori, F.D. Marzo, R. Cennamo, G. Porto, L. Zeni, Proof of concept for a quick and highly sensitive on-site detection of SARS-CoV-2 by plasmonic optical fibers and molecularly imprinted polymers, Sensors 21 (2021) 1681. https://doi.org/10.3390/s21051681.
[11] T. Muhammad, O. Yimit, Y. Turahun, K. Muhammad, Y. Uludag, Z. Zhao, On-line determination of 4-nitrophenol by combining molecularly imprinted solid-phase extraction and fiber-optic spectrophotometry, J. Separ. Sci. 37 (2014) 1873–1879. https://doi.org/10.1002/jssc.201400211.
[12] Y. Hu, T. Muhammad, B. Wu, A. Wei, X. Yang, L. Chen, A simple on-line detection system based on fiber-optic sensing for the realtime monitoring of fixed bed adsorption processes of molecularly imprinted polymers, J. Chromatogr. A 1622 (2020) 461112. https://doi.org/10.1016/j.chroma.2020.461112.
[13] X. Yang, T. Muhammad, J. Yang, A. Yasen, L. Chen, In-situ kinetic and thermodynamic study of 2,4-dichlorophenoxyacetic acid adsorption on molecularly imprinted polymer based solid-phase microextraction coatings, Sens. Actuator A Phys. 313 (2020) 112190. https://doi.org/10.1016/j.sna.2020.112190.
[14] D. Kriz, O. Ramström, A. Svenssön, K. Mosbach, Introducing biomimetic sensors based on molecularly imprinted polymers as recognition elements, Anal. Chem. 67 (1995) 2142–2144. https://doi.org/10.1021/ac00109a037.
[15] S.M. Ng, R. Narayanaswamy, Fluorescence sensor using a molecularly imprinted polymer as a recognition receptor for the detection of aluminium ions in aqueous media, Anal. Bioanal. Chem. 386 (2006) 1235–1244. https://doi.org/10.1007/s00216-006-0736-3.
[16] S.M. Ng, R. Narayanaswamy, Molecularly imprinted β-cyclodextrin polymer as potential optical receptor for the detection of organic compound, Sensor. Actuator. B Chem. 139 (2009) 156–165. https://doi.org/10.1016/j.snb.2008.10.035.
[17] H. Sun, J. Lai, D. Lin, X. Huang, Y. Zuo, Y. Li, A novel fluorescent multifunctional monomer for preparation of silver ion-imprinted fluorescent on–off chemosensor, Sensor. Actuator. B Chem. 224 (2016) 485–491. https://doi.org/10.1016/j.snb.2015.10.052.
[18] D. Pan, M. Xun, H. Lan, J. Li, Z. Wu, Y. Guo, Selective, sensitive, and fast determination of S-layer proteins by a molecularly imprinted photonic polymer coated film and a fiber-optic spectrometer, Anal. Bioanal. Chem. 411 (2019) 7737–7745. https://doi.org/10.1007/s00216-019-02109-1.
[19] X. Liu, H. Fang, L. Yu, Molecularly imprinted photonic polymer based on beta-cyclodextrin for amino acid sensing, Talanta 116 (2013) 283–289. https://doi.org/10.1016/j.talanta.2013.05.003.
[20] Y. Cao, G. Liu, X. Qin, H. Li, C. Liu, Preparation and application of 2-chlorophenol molecularly imprinted photonic crystal hydrogel sensor, J. Macromol. Sci. A. 58 (2020) 336–343. https://doi.org/10.1080/10601325.2020.1854046.
[21] S. Chen, H. Sun, Z. Huang, Z. Jin, S. Fang, J. He, Y. Liu, Y. Zhang, J. Lai, The visual detection of anesthetics in fish based on an inverse opal photonic crystal sensor, RSC Adv. 9 (2019) 16831–16838. https://doi.org/10.1039/C9RA01600G.
[22] Y. Zhang, Z. Jin, Q. Zeng, Y. Huang, H. Gu, J. He, Y. Liu, S. Chen, H. Sun, J. Lai, Visual test for the presence of the illegal additive ethyl anthranilate by using a photonic crystal test strip, Mikrochim. Acta 186 (2019) 685. https://doi.org/10.1007/s00604-019-3800-3.
[23] T. Kamra, S. Chaudhary, C. Xu, L. Montelius, J. Schnadt, L. Ye, Covalent immobilization of molecularly imprinted polymer nanoparticles on a gold surface using carbodiimide coupling for chemical sensing, J. Colloid Interface Sci. 461 (2016) 1–8. https://doi.org/10.1016/j.jcis.2015.09.009.
[24] L. Shang, C. Liu, M. Watanabe, B. Chen, K. Hayashi, LSPR sensor array based on molecularly imprinted sol-gels for pattern recognition of volatile organic acids, Sensor. Actuator. B Chem. 249 (2017) 14–21. https://doi.org/10.1016/j.snb.2017.04.048.
[25] B. Chen, H. Guo, C. Liu, L. Shang, X. Ye, L. Chen, C. Feng, K. Hayashi, Molecularly imprinted sol-gel/Au@Ag core-shell nano-urchin localized surface plasmon resonance sensor designed in reflection mode for detection of organic acid vapors, Biosens. Bioelectron. 169 (2020) 112639. https://doi.org/10.1016/j.bios.2020.112639.
[26] Y. He, J. Lai, H. Sun, Z. Chen, S. Lan, A fast, sensitive and stable fluorescent fiber-optic chemosensor for quantitative detection of Fe^{3+} in real water and HepG2 living cells, Sensor. Actuator. B Chem. 225 (2016) 405–412. https://doi.org/10.1016/j.snb.2015.11.048.
[27] Q. Li, S. Shinde, G. Grasso, A. Caroli, R. Abouhany, M. Lanzillotta, G. Pan, W. Wan, K. Rurack, B. Sellergren, Selective detection of phospholipids using molecularly imprinted fluorescent sensory core-shell particles, Sci. Rep. 10 (2020) 9924. https://doi.org/10.1038/s41598-020-66802-3.
[28] A.L. Jenkins, R. Yin, J.L. Jensen, Molecularly imprinted polymer sensors for pesticide and insecticide detection in water, Analyst 126 (2001) 798–802. https://doi.org/10.1039/b008853f.
[29] T.H. Nguyen, S.A. Hardwick, T. Sun, K.T.V. Grattan, Intrinsic fluorescence-based optical fiber sensor for cocaine using a molecularly imprinted polymer as the recognition element, IEEE Sensor. J. 12 (2012) 255–260. https://doi.org/10.1109/JSEN.2011.2158537.
[30] X. Ton, B. Tse Sum Bui, M. Resmini, P. Bonomi, I. Dika, O. Soppera, K. Haupt, A versatile fiber-optic fluorescence sensor based on molecularly imprinted microstructures polymerized in situ, Angew Chem. Int. Ed. Engl. 52 (2013) 8317–8321. https://doi.org/10.1002/anie.201301045.
[31] Y. Xiong, Z. Ye, J. Xu, Y. Liu, H. Zhang, A microvolume molecularly imprinted polymer modified fiber-optic evanescent wave sensor for bisphenol A determination, Anal. Bioanal. Chem. 406 (2014) 2411–2420. https://doi.org/10.1007/s00216-014-7664-4.
[32] S. Carrasco, E. Benito-Pena, D.R. Walt, M.C. Moreno-Bondi, Fiber-optic array using molecularly imprinted microspheres for antibiotic analysis, Chem. Sci. 6 (2015) 3139–3147. https://doi.org/10.1039/C5SC00115C.
[33] Y. Zhu, M. Cui, J. Ma, Q. Zhang, Fluorescence detection of d-aspartic acid based on thiol-ene cross-linked molecularly imprinted optical fiber probe, Sensor. Actuator. B Chem. 305 (2020) 127323. https://doi.org/10.1016/j.snb.2019.127323.
[34] Q. Huang, C. Lv, X. Yuan, M. He, J. Lai, H. Sun, A novel fluorescent optical fiber sensor for highly selective detection of antibiotic ciprofloxacin based on replaceable molecularly imprinted nanoparticles composite hydrogel detector, Sensor. Actuator. B Chem. 328 (2021) 129000. https://doi.org/10.1016/j.snb.2020.129000.
[35] R. Verma, B.D. Gupta, Fiber optic SPR sensor for the detection of 3-pyridinecarboxamide (vitamin B3) using molecularly imprinted hydrogel, Sensor. Actuator. B Chem. 177 (2013) 279–285. https://doi.org/10.1016/j.snb.2012.10.135.
[36] N. Cennamo, G. D'Agostino, M. Pesavento, L. Zeni, High selectivity and sensitivity sensor based on MIP and SPR in tapered plastic optical fibers for the detection of l-nicotine, Sensor. Actuator. B Chem. 191 (2014) 529–536. https://doi.org/10.1016/j.snb.2013.10.067.
[37] N. Cennamo, A. Donà, P. Pallavicini, G. D'Agostino, G. Dacarro, L. Zeni, M. Pesavento, Sensitive detection of 2,4,6-trinitrotoluene by tridimensional monitoring of molecularly imprinted polymer with optical fiber and five-branched gold nanostars, Sensor. Actuator. B Chem. 208 (2015) 291–298. https://doi.org/10.1016/j.snb.2014.10.079.
[38] H. Agrawal, A.M. Shrivastav, B.D. Gupta, Surface plasmon resonance based optical fiber sensor for atrazine detection using molecular imprinting technique, Sensor. Actuator. B Chem. 227 (2016) 204–211. https://doi.org/10.1016/j.snb.2015.12.047.
[39] A.M. Shrivastav, S.K. Mishra, B.D. Gupta, Fiber optic SPR sensor for the detection of melamine using molecular imprinting, Sensor. Actuator. B Chem. 212 (2015) 404–410. https://doi.org/10.1016/j.snb.2015.02.028.
[40] A.M. Shrivastav, S.K. Mishra, B.D. Gupta, Localized and propagating surface plasmon resonance based fiber optic sensor for the detection of tetracycline using molecular imprinting, Mater. Res. Express 2 (2015), 035007. https://doi.org/10.1088/2053-1591/2/3/035007.
[41] A.M. Shrivastav, S.P. Usha, B.D. Gupta, A localized and propagating SPR, and molecular imprinting based fiber-optic ascorbic acid sensor using an in situ polymerized polyaniline-Ag nanocomposite, Nanotechnology 27 (2016) 345501. https://doi.org/10.1088/0957-4484/27/34/345501.
[42] A.M. Shrivastav, S.P. Usha, B.D. Gupta, Highly sensitive and selective erythromycin nanosensor employing fiber optic SPR/ERY imprinted nanostructure: application in milk and honey, Biosens. Bioelectron. 90 (2017) 516–524. https://doi.org/10.1016/j.bios.2016.10.041.
[43] N. Cennamo, D. Maniglio, R. Tatti, L. Zeni, A.M. Bossi, Deformable molecularly imprinted nanogels permit sensitivity-gain in plasmonic sensing, Biosens. Bioelectron. 156 (2020) 112126. https://doi.org/10.1016/j.bios.2020.112126.
[44] N. Cennamo, G. D'Agostino, G. Porto, A. Biasiolo, C. Perri, F. Arcadio, L. Zeni, A molecularly imprinted polymer on a plasmonic plastic optical fiber to detect perfluorinated compounds in water, Sensors 18 (2018) 1836. https://doi.org/10.3390/s18061836.
[45] A. Pathak, B.D. Gupta, Ultra-selective fiber optic SPR platform for the sensing of dopamine in synthetic cerebrospinal fluid incorporating permselective nafion membrane and surface imprinted MWCNTs-PPy matrix, Biosens. Bioelectron. 133 (2019) 205–214. https://doi.org/10.1016/j.bios.2019.03.023.
[46] M. Pesavento, L. Zeni, L. De Maria, G. Alberti, N. Cennamo, SPR-optical fiber-molecularly imprinted polymer sensor for the detection of furfural in wine, Biosensors 11 (2021) 72. https://doi.org/10.3390/bios11030072.
[47] S. Lepinay, A. Ianoul, J. Albert, Molecular imprinted polymer-coated optical fiber sensor for the identification of low molecular weight molecules, Talanta 128 (2014) 401–407. https://doi.org/10.1016/j.talanta.2014.04.037.
[48] S. Korposh, I. Chianella, A. Guerreiro, S. Caygill, S. Piletsky, S.W. James, R.P. Tatam, Selective vancomycin detection using optical fibre long period gratings functionalised with molecularly imprinted polymer nanoparticles, Analyst 139 (2014) 2229–2236. https://doi.org/10.1039/c3an02126b.
[49] Á. González-Vila, M. Debliquy, D. Lahem, C. Zhang, P. Mégret, C. Caucheteur, Molecularly imprinted electropolymerization on a metal-coated optical fiber for gas sensing applications, Sensor. Actuator. B Chem. 244 (2017) 1145–1151. https://doi.org/10.1016/j.snb.2017.01.084.
[50] T. Wang, S. Korposh, S. James, S.W. Lee, Long-period grating fiber-optic sensors exploiting molecularly imprinted TiO_2 nanothin films with photocatalytic self-cleaning ability, Mikrochim. Acta 187 (2020) 663. https://doi.org/10.1007/s00604-020-04603-1.
[51] L. Liu, F. Grillo, F. Canfarotta, M. Whitcombe, S.P. Morgan, S. Piletsky, R. Correia, C. He, A. Norris, S. Korposh, Carboxyl-fentanyl detection using optical fibre grating-based sensors functionalised with molecularly imprinted nanoparticles, Biosens. Bioelectron. 177 (2021) 113002. https://doi.org/10.1016/j.bios.2021.113002.

[52] S.-W. Lee, S. Ahmed, T. Wang, Y. Park, S. Matsuzaki, S. Tatsumi, S. Matsumoto, S. Korposh, S. James, Label-free creatinine optical sensing using molecularly imprinted titanium dioxide-polycarboxylic acid hybrid thin films: a preliminary study for urine sample analysis, Chemosensors 9 (2021) 185. https://doi.org/10.3390/chemosensors9070185.
[53] R.B. Queiros, S.O. Silva, J.P. Noronha, O. Frazao, P. Jorge, G. Aguilar, P.V. Marques, M.G. Sales, Microcystin-LR detection in water by the Fabry-Pérot interferometer using an optical fibre coated with a sol-gel imprinted sensing membrane, Biosens. Bioelectron. 26 (2011) 3932–3937. https://doi.org/10.1016/j.bios.2011.03.015.
[54] A.M. Shrivastav, G. Sharma, R. Jha, Hypersensitive and selective biosensing based on microfiber interferometry and molecular imprinted nanoparticles, Biosens. Bioelectron. 141 (2019) 111347. https://doi.org/10.1016/j.bios.2019.111347.
[55] X. Liu, W. Lin, P. Xiao, M. Yang, L.-P. Sun, Y. Zhang, W. Xue, B.-O. Guan, Polydopamine-based molecular imprinted optic microfiber sensor enhanced by template-mediated molecular rearrangement for ultra-sensitive C-reactive protein detection, Chem. Eng. J. 387 (2020) 124074. https://doi.org/10.1016/j.cej.2020.124074.
[56] S.P. Usha, A.M. Shrivastav, B.D. Gupta, A contemporary approach for design and characterization of fiber-optic-cortisol sensor tailoring LMR and ZnO/PPY molecularly imprinted film, Biosens. Bioelectron. 87 (2017) 178–186. https://doi.org/10.1016/j.bios.2016.08.040.
[57] S.P. Usha, B.D. Gupta, Urinary *p*-cresol diagnosis using nanocomposite of ZnO/MoS_2 and molecular imprinted polymer on optical fiber based lossy mode resonance sensor, Biosens. Bioelectron. 101 (2018) 135–145. https://doi.org/10.1016/j.bios.2017.10.029.
[58] N. Cennamo, G. Testa, S. Marchetti, L. De Maria, R. Bernini, L. Zeni, M. Pesavento, Intensity-based plastic optical fiber sensor with molecularly imprinted polymer sensitive layer, Sensor. Actuator. B Chem. 241 (2017) 534–540. https://doi.org/10.1016/j.snb.2016.10.104.
[59] A.M. Shrivastav, S.K. Mishra, B.D. Gupta, Surface plasmon resonance-based fiber optic sensor for the detection of ascorbic acid utilizing molecularly imprinted polyaniline film, Plasmonics 10 (2015) 1853–1861. https://doi.org/10.1007/s11468-015-0005-4.
[60] N. Cennamo, G. D'Agostino, R. Galatus, L. Bibbò, M. Pesavento, L. Zeni, Sensors based on surface plasmon resonance in a plastic optical fiber for the detection of trinitrotoluene, Sensor. Actuator. B Chem. 188 (2013) 221–226. https://doi.org/10.1016/j.snb.2013.07.005.
[61] N. Cennamo, L. De Maria, G. D'Agostino, M. Pesavento, L. Zeni, Combined molecularly imprinted polymer and surface plasmon resonance transduction in plastic optical fiber for monitoring oil-filled power transformers, Procedia Eng. 87 (2014) 532–535. https://doi.org/10.1016/j.proeng.2014.11.541.
[62] M.V. Foguel, X.-A. Ton, M.V.B. Zanoni, M.D.P.T. Sotomayor, K. Haupt, B. Tse Sum Bui, A molecularly imprinted polymer-based evanescent wave fiber optic sensor for the detection of basic red 9 dye, Sensor. Actuator. B Chem. 218 (2015) 222–228. https://doi.org/10.1016/j.snb.2015.05.007.
[63] X.A. Ton, V. Acha, P. Bonomi, B. Tse Sum Bui, K. Haupt, A disposable evanescent wave fiber optic sensor coated with a molecularly imprinted polymer as a selective fluorescence probe, Biosens. Bioelectron. 64 (2015) 359–366. https://doi.org/10.1039/C3AN01098H.
[64] R. Verma, B.D. Gupta, Optical fiber sensor for the detection of tetracycline using surface plasmon resonance and molecular imprinting, Analyst 138 (2013) 7254–7263.
[65] F.d.L. Meza López, S. Khan, G. Picasso, M.D.P.T. Sotomayor, A novel highly sensitive imprinted polymer-based optical sensor for the detection of Pb(II) in water samples, Environ. Nanotechnol. Monit. Manag. 16 (2021) 100497. https://doi.org/10.1016/j.enmm.2021.100497.
[66] K. Peters, Polymer optical fiber sensors-a review, Smart Mater. Struct. 20 (2011), 013002. https://doi.org/10.1088/0964-1726/20/1/013002.
[67] R. Min, Z. Liu, L. Pereira, C. Yang, Q. Sui, C. Marques, Optical fiber sensing for marine environment and marine structural health monitoring: a review, Opt Laser. Technol. 140 (2021) 107082. https://doi.org/10.1016/j.optlastec.2021.107082.
[68] N. Cennamo, L. De Maria, G. D'Agostino, L. Zeni, M. Pesavento, Monitoring of low levels of furfural in power transformer oil with a sensor system based on a POF-MIP platform, Sensors 15 (2015) 8499–8511. https://doi.org/10.3390/s150408499.
[69] H. Abduldaem Mohammed, M. Hanif Yaacob, Modified single mode optical fiber ammonia sensors deploying PANI thin films, in: S.W. Harun (Editor), Application of Optical Fiber in Engineering, IntechOpen, London, 2020.
[70] S.P. Wren, T.H. Nguyen, P. Gascoine, R. Lacey, T. Sun, K.T.V. Grattan, Preparation of novel optical fibre-based cocaine sensors using a molecular imprinted polymer approach, Sensor. Actuator. B Chem. 193 (2014) 35–41. https://doi.org/10.1016/j.snb.2013.11.071.
[71] M. Chauhan, V. Kumar Singh, Review on recent experimental SPR/LSPR based fiber optic analyte sensors, Opt. Fiber Technol. 64 (2021) 102580. https://doi.org/10.1016/j.yofte.2021.102580.
[72] A.K. Sharma, R. Jha, B.D. Gupta, Fiber-optic sensors based on surface plasmon resonance: a comprehensive review, IEEE Sensor. J. 7 (2007) 1118–1129. https://doi.org/10.1109/JSEN.2007.897946.
[73] N. Cennamo, P. Zuppella, D. Bacco, A.J. Corso, M.G. Pelizzo, L. Zeni, SPR sensor platform based on a novel metal bilayer applied on D–shaped plastic optical fibers for refractive index measurements in the range 1.38-1.42, IEEE Sensor. J. 16 (2016) 4822–4827. https://doi.org/10.1109/JSEN.2016.2549271.
[74] F. Chiavaioli, F. Baldini, S. Tombelli, C. Trono, A. Giannetti, Biosensing with optical fiber gratings, Nanophotonics 6 (2017) 663–679. https://doi.org/10.1515/nanoph-2016-0178.
[75] Z. Chen, Y. Luo, C. Huang, X. Shen, In situ assembly of ZnO/graphene oxide on synthetic molecular receptors: towards selective photoreduction of Cr(VI) via interfacial synergistic catalysis, Chem. Eng. J. 414 (2021) 128914. https://doi.org/10.1016/j.cej.2021.128914.
[76] J.S. Santos, I.M. Raimundo, C.M.B. Cordeiro, C.R. Biazoli, C.A.J. Gouveia, P.A.S. Jorge, Characterisation of a Nafion film by optical fibre Fabry-Pérot interferometry for humidity sensing, Sensor. Actuator. B Chem. 196 (2014) 99–105. https://doi.org/10.1016/j.snb.2014.01.101.
[77] V. Bhardwaj, K. Kishor, A.C. Sharma, Tapered optical fiber geometries and sensing applications based on Mach-Zehnder Interferometer: a review, Opt. Fiber Technol. 58 (2020) 102302. https://doi.org/10.1016/j.yofte.2020.102302.
[78] S.A. Pidenko, N.A. Burmistrova, A.A. Shuvalov, A.A. Chibrova, Y.S. Skibina, I.Y. Goryacheva, Microstructured optical fiber-based luminescent biosensing: is there any light at the end of the tunnel?-A review, Anal. Chim. Acta 1019 (2018) 14–24. https://doi.org/10.1016/j.aca.2017.12.010.
[79] I. Del Villar, F.J. Arregui, C.R. Zamarreño, J.M. Corres, C. Bariain, J. Goicoechea, C. Elosua, M. Hernaez, P.J. Rivero, A.B. Socorro, A. Urrutia, P. Sanchez, P. Zubiate, D. Lopez, N. De Acha, J. Ascorbe, I.R. Matias, Optical sensors based on lossy-mode resonances, Sensor. Actuator. B Chem. 240 (2017) 174–185. https://doi.org/10.1016/j.snb.2016.08.126.